Investigation and Mitigation of Radio Frequency Interference Caused by Weak Grounding of USB Type-C Receptacle Connector

Anfeng Huang[1], Xin Yan[2], Jingdong Sun[3], Qiaolei Huang[4] and Jun Fan[10]
EMC Laboratory
Missouri University of Science and Technology
Rolla, MO, USA
jfan@mst.edu

Songping Wu[5], Dave Zhang[6], Huan Liao[7], Shuai Jin[8] and Zhiping Yang[9]
Google Inc.
Mountain View, CA, USA
songpingwu, zhipingyang@google.com

***Abstract*—In modern mobile electronic systems, USB connector has been identified as one of the dominant noise sources for desense issues. In this paper, the noise coupled to the Wi-Fi antenna from a USB connector is investigated. With the assistance of full-wave simulations, the root cause of desense noise is identified as the non-ideal electrical connection between the metal chassis and the USB receptacle shell where it is installed. The proposed radiation mechanism is validated through measurements of a real tablet device, and 15 dB noise level reduction is observed with a better grounding structure.**

***Index Terms*—radiation mechanism, Type-C USB, full-wave simulation, grounding quality evaluation**

I. Introduction

With the increasing complexity and miniaturization of modern mobile platforms, including mobile phones, tablets, and laptops, the distances between antennas and high-speed integrated circuits (ICs) or connectors are driven closer, which intensify the radio frequency interference (RFI) issue. In addition, the ever-growing demands for higher data transfer rate make the matter worse. As discussed in [1], the noise could be generated by different noise sources, such as liquid-crystal displays [2], digital microphones [3] and switching power supplies [4].

Universal serial bus (USB) connector is one of the dominant noise sources among different designs and products as reported in [5]. Even though the signal propagation in USB connectors is designed to be differential, the undesired radiation generated by the USB connectors or corresponding traces is inevitable. Moreover, with the emerging of USB 3.0 technology which operates at 5 Gbps, it has been shown that noise due to the USB 3.0 data spectrum can radiate from receptacle connectors and coupled to the receiving antennas for wireless communication, such as the 2.4 GHz frequency band Wi-Fi and Bluetooth. It increases the noise floor of the receiver and degrades the sensitivity of the antenna by dozens of dB.

Recently, several practical solutions have been proposed to reduce the noise generated by the USB data transfer. In [6], the radiation brought by shell grounding between plug and receptacle connectors was investigated. The desensitization issue caused by the USB 3.0 data transfer was greatly mitigated as extra ground contacts were added. Another practical solution was demonstrated in [7] by shielding the back-side of USB receptacle connector, and the noise radiation mechanism was analyzed by an equivalent dipole moment. Even though the noise radiation mechanism was extensively studied, the aforementioned methods were only validated for Type-A connectors. In addition, the noises in those cases are directly generated by exposed USB 3.0 signal pins in USB connectors.

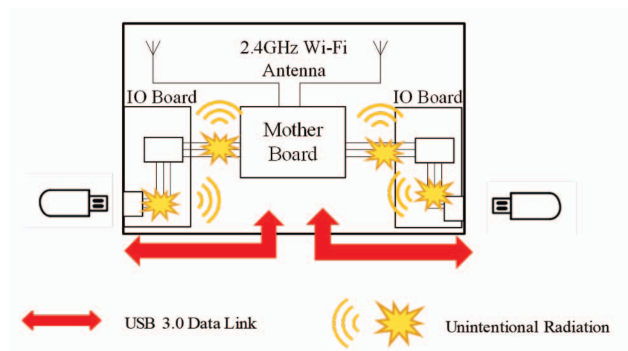

Fig. 1. Illustration for desensitization issue caused by USB 3.0 data transfer.

As the USB technology continuously evolves to Type-C, more severe RFI problems are expected in real applications, due to the higher data transfer capability and smaller size. In addition, the unifying of data, video, and power delivery within one single connector may introduce more interferences in real designs. A thorough search of the relevant studies yielded to very limited investigations regarding the RFI issues caused by USB Type-C connectors.

In this paper, the structure of a Type-C receptacle connector design is demonstrated. Due to the limitations of space and routing, the signal traces in USB receptacle connector are separated into surface mount and through hole ones. The noise

978-1-7281-7430-3/20/$31.00 ©2020 IEEE

contributed by the two types of pins are analyzed. Besides, the noise radiation mechanism is identified as the weak grounding connection between the receptacle connector and the metal chassis. We note the noise is generated by the installation configuration but not the connector itself. Eventually, a noise mitigation method is proposed and validated using a real tablet product. Correspondingly, 15 dB noise reduction is achieved by improving the grounding structure between the tablet chassis and the USB receptacle connector.

II. Noise Source Identification

As discussed in [6], USB 3.0 has a 5 Gbit/s signaling rate, which could be modeled as a sinc function due to data scrambling. The spectrum of USB signal ranges from DC to the first data null at 5 GHz. The boardband noise emitted from the USB device can affect the signal to noise ratio and limit the sensitivity of Wi-Fi receiver. Fig. 2 shows the time domain waveform and data spectrum measured by directly probing one of the USB 3.0 transmit-pair signals of the device under test (DUT).

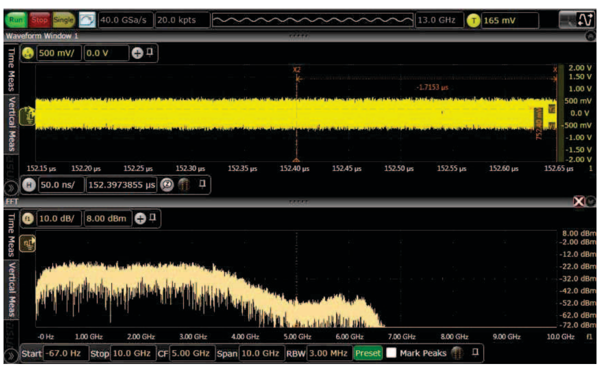

Fig. 2. Waveform and spectrum of USB 3.0 data.

A. Noise Comparison of USB Data Transfer in Idle and Active States

To identify whether the desense noise is caused by USB data transfer, the noise levels are measured as USB flash drive are in idle and active states.

To evaluate the noise coupled to Wi-Fi antenna, direct noise measurement was conducted, where the Wi-Fi antenna was connected to spectrum analyzer (Model: R&S FSV-30) with low noise amplifier (Model: MiniCircuits ZX60-P103LN+ and ZX60-6013E-S+). DUT and instruments were placed inside a 3 m semi-anechoic chamber to eliminate the influence of extra Wi-Fi band noise as shown in Fig. 3. Noise coupled to the antenna is compared as USB flash drive is in idle and active states, as demonstrated in Fig. 4. Note that the Type-C plug side contains two differential pairs for high-speed USB data transfer. And only the results for TX1/RX1 pair are illustrated as an example.

It could be observed that no noise is generated by the DUT when USB flash drive is in the idle state. And the noise received by the Wi-Fi antenna increases by ∼15 dB as the

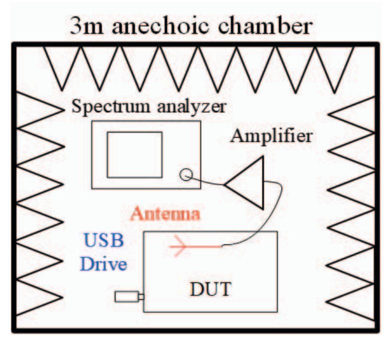

Fig. 3. Measurement setup for noise caused by USB 3.0 flash drive.

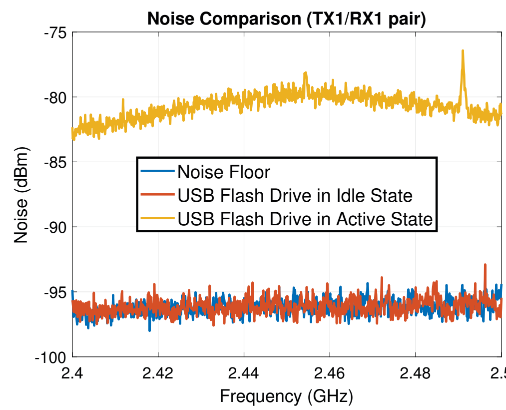

Fig. 4. Noise level comparison as the USB 3.0 flash drive are in active and idle states.

USB flash drive is operating in super speed active state. Fig. 5 shows the configuration of a commercial tablet where the Type-C receptacle connector serves as the aggressor and Wi-Fi antenna is the victim.

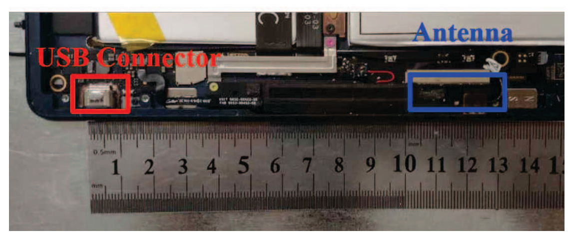

Fig. 5. Type-C receptacle connector (aggressor) and Wi-Fi antenna (victim).

B. Challenges in Further Noise Source Identification

It is confirmed that the dominant noise source is caused by the super speed USB data transfer. However, the USB Type-C connector contains two pairs of full-duplex channels, so the noise contributed by the transmitting and receiving signals could not be separated with USB 3.0 data transfer. In addition, the signal pins are separated into surface mount and through hole types due to the routing limitation. The pin map of USB connector and the corresponding 3D model are demonstrated in Fig. 6 and Fig. 7, respectively. In the design, ”A” class pins are surface mount ones and "B" class pins are through hole ones.

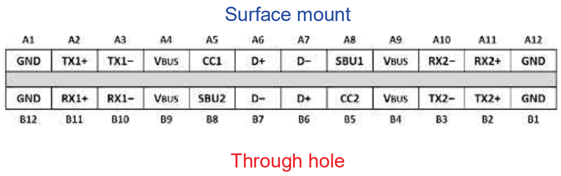

Fig. 6. Pin map of Type-C receptacle connector.

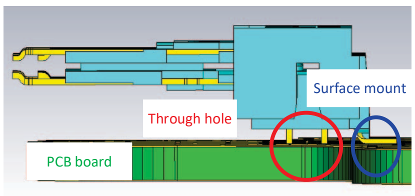

Fig. 7. Illustration of surface and through hole pins.

Due to the different signal traces design, the noise generated by surface mount and through hole pins can not be easily separated and characterized.

III. Dominant Noise Source Investigation

To evaluate the noise generated by the two different pins, a passive measurement setup was built to investigate the noise generated by surface mount and through hole pins, respectively. And the noise coupling between signal traces of Type-C connector and antenna could be defined as the transmission coefficient, i.e. S_{21}. The noise transfer function could be directly used to discriminate the difference between these two types of pins. Further, the measurements can be served as reference for simulation validation.

A. Configuration of Passive Measurement Setup and Simulation Model

The passive measurement setup consists of a vector network analyzer (Model: Keysight N5245A), a Type-C plug to SMA connector fan-out board and the DUT. It is worth noting that to eliminate the direct radiation from the fan-out board to the antenna, embedded stripline is used. In addition, the exposed traces and connector pins are well shielded by solder and copper tapes, as shown in Fig. 8(b). With the passive measurement setup, the transmission coefficient i.e. S_{21} for each pin could be accurately characterized.

To further understand the noise generation mechanism, a full-wave simulation model was built according to the passive measurement setup, as shown in Fig. 9. The simulation model contains all the details of metal chassis, USB connectors, USB board and antenna. We note that only part of the fan-out board was used to accelerate the simulation.

The noise is excited from the fan-out board, where the surface mount and through hole pins could be driven separately. And the victim port is assigned on the Wi-Fi antenna, which is

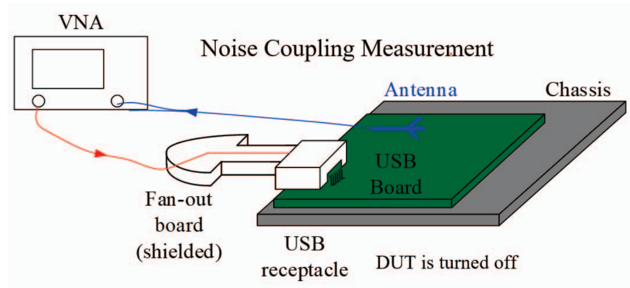

(a)

(b)

Fig. 8. (a) Measurement setup for passive noise transfer function. (b) Shielded Type-C plug to SMA fan-out board.

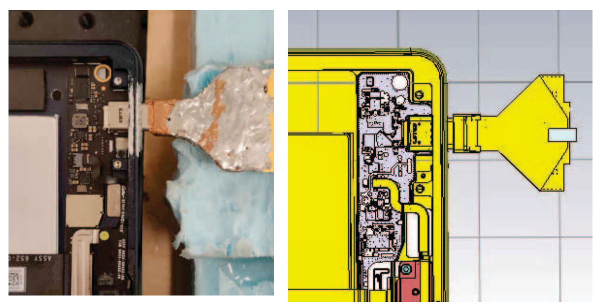

Fig. 9. Illustration of real measurement setup and simulation model.

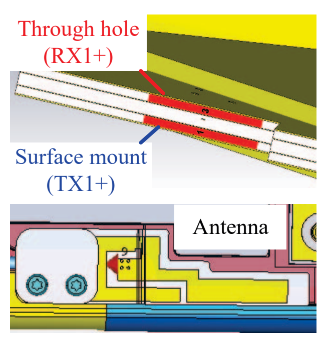

Fig. 10. Port excitations for simulation model.

the same as measurement. The excitations for different ports are demonstrated in Fig. 10.

B. Simulation Model Validation

To reduce the influence of fan-out board, de-embedding was performed to the end of plug connector in both simulation and measurement. Within the frequency of interest, the simulation results are well matched with the measurement results. The average error is less than 2dB. Even though 100MHz shift is observed for high frequency components, the peak value for the S_{21} shows good correlations. The measurement results validate the simulation model.

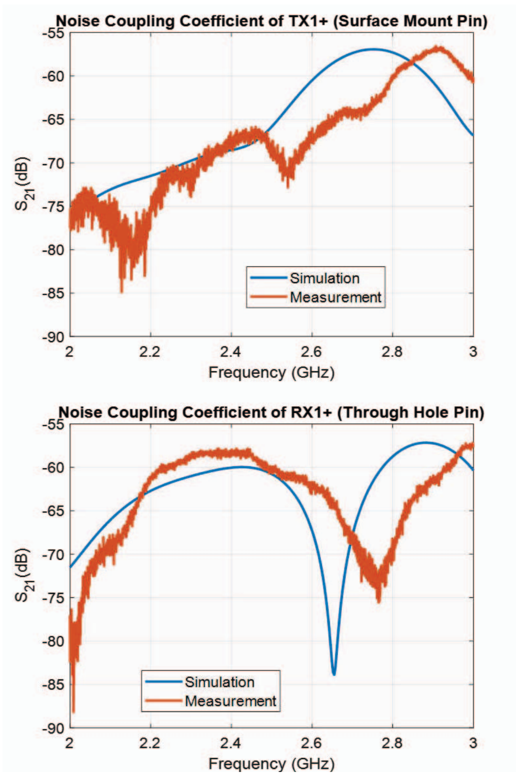

Fig. 11. Measured S_{21} between the Type-C plug and WiFi antenna. Top: surface mount pin. Bottom: through hole pin.

C. Dominant Source Identification

The difference between surface mount pin (TX1+) and through hole pin (RX1+) for Wi-Fi band is plotted in Fig. 12. Noise generated by through hole pin is ~ 8 dB higher than that of surface mount pin. Based on the simulation results, it can be concluded that through hole pins could generated higher noise in the antenna. In addition, the difference between surface mount and through hole pins needs further investigation.

IV. Dominant Noise Source Investigation

A. Magnetic Field Distribution

To further investigate the differences between two types of pin structure, the H field distribution around the USB receptacle connector is simulated and compared in Fig. 13.

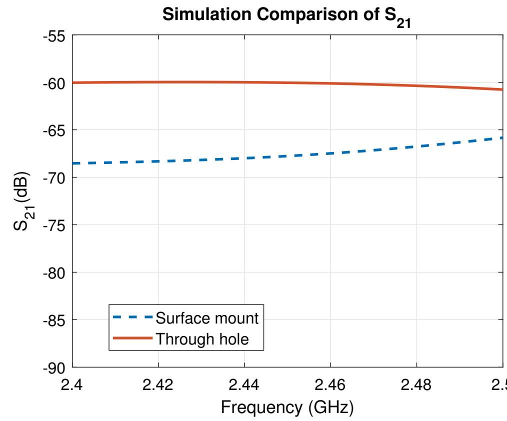

Fig. 12. Simulated noise transfer function comparison between surface mount and through hole pins.

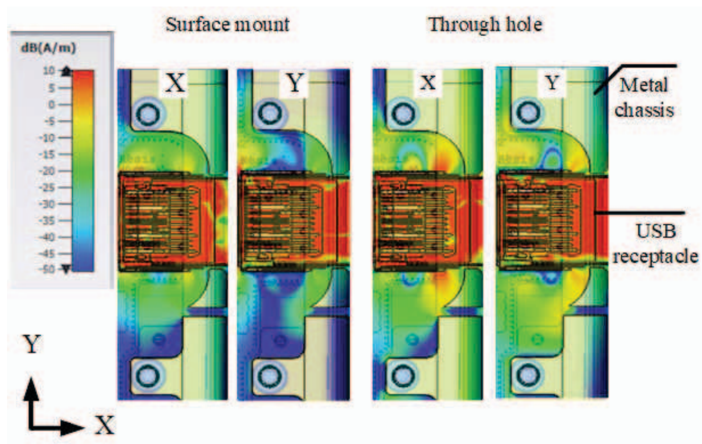

Fig. 13. Simulated H_x and H_y comparison between surface mount and through hole pins.

As shown in the simulation results, the main difference between the two type of pins is H fields along the metal chassis and at two sides of receptacle connector. It is illustrated in Fig. 13, both H_x and H_y generated by through pin are higher than those of surface mount pin. Even though the Wi-Fi antenna is installed 12 cm away from the USB receptacle connector, the noise could still be coupled to the antenna with H field generated along the metal chassis.

B. Radiation Mechanism Investigation

One typical reason for magnetic field generated along chassis is the weak grounding between the connector and the metal chassis where it is installed. To validate this proposal, an extra grounding structure is applied to the metal chassis and receptacle connector as demonstrated in Fig. 14. The simulated current distribution along the chassis with through hole pin excitation is demonstrated in Fig. 15. It can be seen that the current distribution along the chassis wall is drastically reduced with the extra grounding, which validates our proposal.

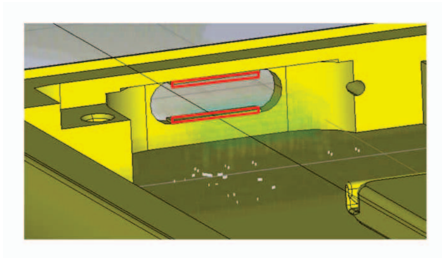

Fig. 14. Full-wave simulation model with extra grounding structure.

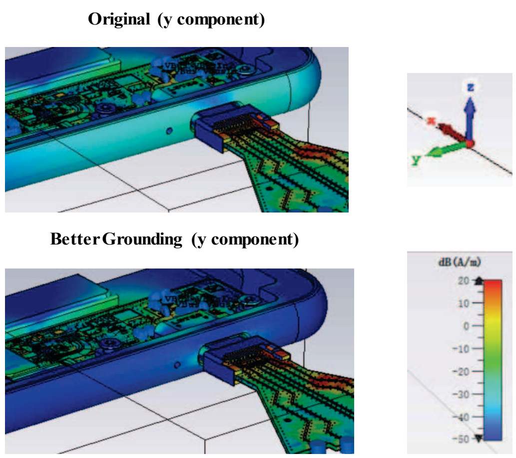

Fig. 15. Current distribution along outer wall of chassis for through hole pin excitation.

In addition, the E field distribution at the cross section of the USB receptacle connector is demonstrated to further reveal the noise radiation mechanism. E-field line starting from the signal trace and ending at the receptacle shell is generated by the signal injected into through hole pin, as shown in Fig. 16. The E-field is also observed between metal chassis and USB receptacle shell, due to the weak grounding connection between them. As the results, an extra current return path is generated by the weak grounding structure, and the current is leaked to the chassis outer wall.

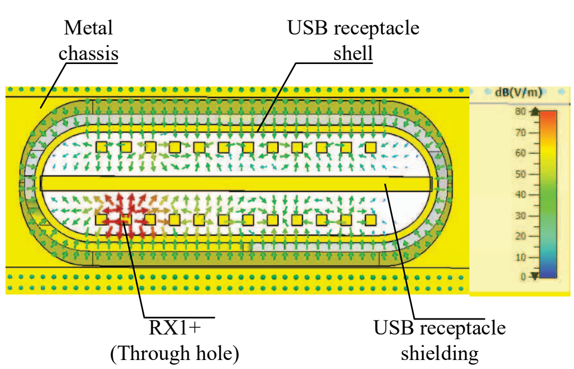

Fig. 16. E field distribution between metal chassis and USB receptacle shell with original grounding configuration. Direction of the conduction current is into the plane.

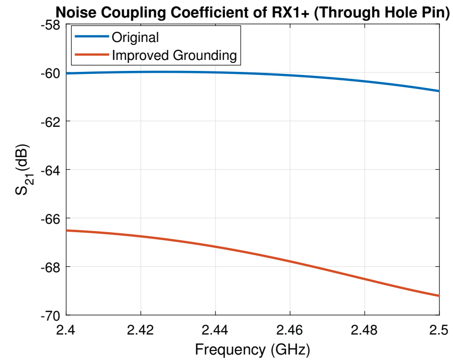

Fig. 17. Comparison for noise coupling coefficient with and without the improved grounding structure.

Eventually the noise coupling coefficient, i.e. S_{21}, is compared with and without the extra grounding structure. Within the frequency of interest (2.4 GHz $\sim$ 2.5 GHz), 7 $\sim$ 9 dB reduction is observed. In summary, it can be concluded that the noise is generated by the weak grounding between metal chassis and USB receptacle connector where it is installed.

V. Noise Mitigation Method and Measurement Validation

A. *Noise Level Mitigation*

To examine noise generated by grounding between tablet chassis and receptacle shell, the whole USB board is removed from the DUT. As demonstrated in Fig. 18, the USB connector and its motherboard are connected to the tablet chassis with conductive tapes. Even though the chassis is made of aluminum, however, it is coated with non-conductive painting, which is electrically isolated with the receptacle connector. Diagram of grounding condition is demonstrated in Fig. 19. Equivalent noise sources could be generated between the weak grounding structures.

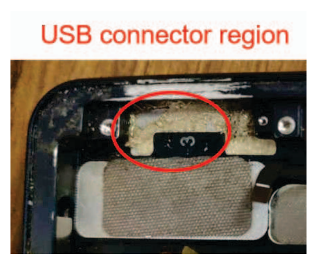

Fig. 18. Electric connection between USB board and chassis.

B. *Measurement Validation*

To verify the radiation, a H field probe resonant at 2.45 GHz is used for noise source identification for both original and improved grounding structures. The scanning is done with USB 3.0 data transferring and results are shown in Fig. 20. Note that the non-conductive coating is removed and replaced

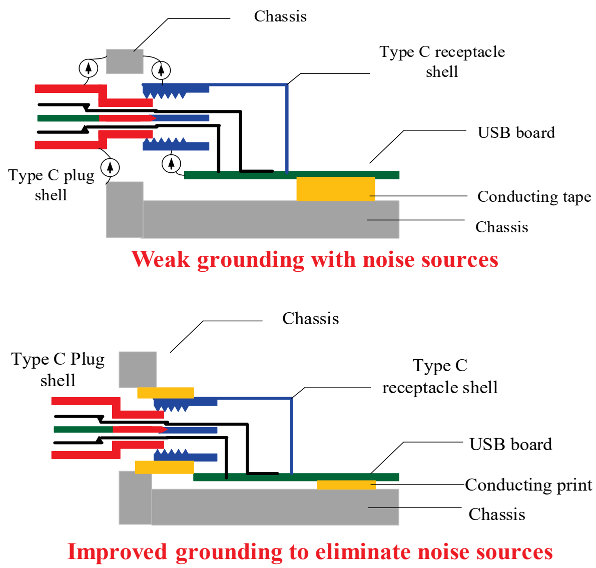

Fig. 19. Diagram of original and improved grounding connection for DUT.

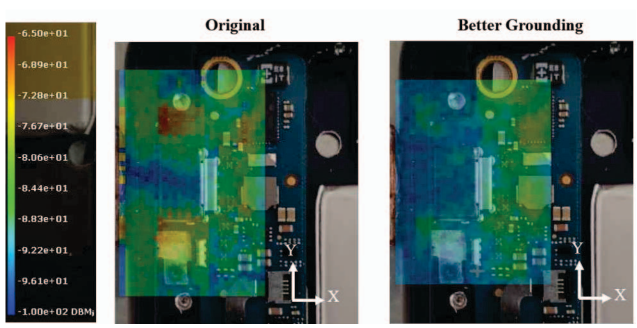

Fig. 20. Comparison for H_x field pattern of origin grounding (left-hand side) and improved grounding (right-hand side) at 2.45 GHz.

by silver print and an extra screw is used to enhance the mechanical strength.

As we have demonstrated in previous section, it is expected that the H_x components generated along the chassis wall would be much larger than those of H_y. Therefore, the H_x field distribution around the USB receptacle connector is measured for validation.

It is clear that large H_x field is observed at two sides of the receptacle connector for the original grounding configuration. In addition, noise field is also observed at the plug side of the connector and along the chassis wall. After receptacle connector is well-grounded to the metal chassis, both plug and receptacle side H_x fields are eliminated. Therefore, we can conclude that the noise is generated by the weak grounding between chassis and receptacle.

As the golden standard for noise reduction verification, the desense noise is directly compared with and without extra grounding as demonstrated in Fig. 21. The noise brought by the USB data transfer is almost eliminated by the improved grounding between chassis and USB receptacle, i.e. 15 dB noise reduction is achieved with the grounding, which further validates the proposal.

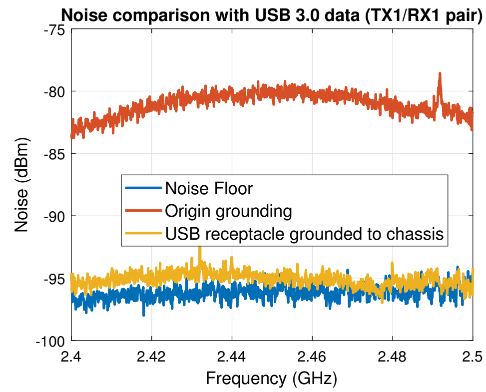

Fig. 21. Comparison of desense noise under original grounding and enhanced grounding.

VI. Conclusion

To evaluate the influence of different pin structure regarding noise generation, a full-wave simulation model is built with the help of the simulation model. The root cause of desense issue is identified as the weak grounding between USB receptacle connector and metal chassis. The simulation results are validated by measurements and a 15 dB noise level reduction is achieved as better grounding structure is provided, which validates the proposed radiation mechanism.

References

[1] Han, Dong-Ho, et al. ”PC client platform RFI risks and mitigation methodologies.” 2015 IEEE Symposium on Electromagnetic Compatibility and Signal Integrity. IEEE, 2015.

[2] Huang, Qiaolei, et al. ”Physics-based dipole moment source reconstruction for RFI on a practical cellphone.” IEEE Transactions on Electromagnetic Compatibility 59.6 (2017): 1693-1700.

[3] Zhong, Yang, et al. ”Measurement-Based Quantification of Buzz Noise in Wireless Devices.” 2019 Joint International Symposium on Electromagnetic Compatibility, Sapporo and Asia-Pacific International Symposium on Electromagnetic Compatibility (EMC Sapporo/APEMC). IEEE, 2019.

[4] Kim, Kiyeong, et al. ”SMPS noise managing methodology for RFI solution in mobile platforms.” 2016 IEEE Electrical Design of Advanced Packaging and Systems (EDAPS). IEEE, 2016.

[5] Davuluri, Pujitha, et al. ”Gb/s USB: RFI risk analysis and test methodologies.” 2015 IEEE Symposium on Electromagnetic Compatibility and Signal Integrity. IEEE, 2015.

[6] Davuluri, Pujitha, and Chung-hao Chen. ”Radio frequency interference due to USB3 connector radiation.” 2013 IEEE International Symposium on Electromagnetic Compatibility. IEEE, 2013.

[7] Sun, Yin, et al. ”Mechanism and Validation of USB 3.0 Connector Caused Radio Frequency Interference.” IEEE Transactions on Electromagnetic Compatibility (2019).